

## CONOIDAL CRACK WITH ELLIPTIC BASES, WITHIN CUBIC CRYSTALS, UNDER ARBITRARILY APPLIED LOADINGS - III. APPLICATION TO BRITTLE FRACTURE SYSTEMS OF $\text{CoSi}_2$ SINGLE CRYSTALS

P. N. B. ANONGBA

Université F.H.B. de Cocody, U.F.R. Sciences des Structures de la Matière et de Technologie, 22 BP 582 Abidjan 22, Côte d'Ivoire

(reçu le 02 Juillet 2024; accepté le 05 Novembre 2024)

\* Correspondance, e-mail : [anongba@gmail.com](mailto:anongba@gmail.com)

### ABSTRACT

Brittle fracture systems ( $\langle 112 \rangle \{111\}$ ,  $\langle 113 \rangle \{110\}$ ,  $\langle 411 \rangle \{122\}$ ) observed in  $\text{CoSi}_2$  single crystals have been confronted to the theoretical analysis of *Part I* of this study. These do correspond to positive local average  $\langle G \rangle$  maxima, where the quantity  $\langle G \rangle$  is the crack extension force  $G$  per unit length of the crack front, averaged over all the positions on the crack front. Hence, equilibrium crack systems provided by the theory are those observed experimentally. Both twinning and cracking systems are of the type  $\langle 112 \rangle \{111\}$  as expected. It is understood that above results are achieved within the framework of the theory of linear elasticity incorporating dislocations as crystal defects and basic elements in the mathematical treatment of fracture.

**Keywords:** *fracture mechanics, linear elasticity, dislocations, crack extension force, high temperature mechanical twinning.*

### RÉSUMÉ

**Fissure conoïdale à base elliptique dans un cristal cubique sous sollicitations extérieures arbitraires – III. Application aux systèmes de fissuration de monocristaux de  $\text{CoSi}_2$**

Les systèmes de fissuration fragile ( $\langle 112 \rangle \{111\}$ ,  $\langle 113 \rangle \{110\}$ ,  $\langle 411 \rangle \{122\}$ ) observés dans des monocristaux de  $\text{CoSi}_2$  ont été confrontés à l'analyse théorique de la première partie de cette étude. Ceux-ci correspondent à des maxima moyens locaux positifs  $\langle G \rangle$ , où la quantité  $\langle G \rangle$  est la force d'extension de la fissure  $G$  par unité de longueur du front de fissure, moyennée

P. N. B. ANONGBA

sur toutes les positions sur le front de fissure. Par conséquent, les systèmes de fissures à l'équilibre fournis par la théorie sont ceux observés expérimentalement. Les systèmes de maclage et de fissuration sont du type  $\langle 112 \rangle \{111\}$  comme prévu. Il est entendu que les résultats ci-dessus sont obtenus dans le cadre de la théorie de l'élasticité linéaire intégrant les dislocations en tant que défauts cristallins et éléments de base dans le traitement mathématique de la fracture.

**Mots-clés :** *mécanique de la rupture, élasticité linéaire, dislocation, force d'extension de fissure, maclage mécanique à haute température*

## I - INTRODUCTION

In the first part of this study [1], we have considered a conoidal nucleus of crack (vertex  $O$ ) within an infinitely extended cubic material, arbitrarily oriented ( $O; x'_j$ ) with respect to the laboratory reference frame ( $O; x_j$ ); the latter indicates the directions  $x_j$  of the externally applied loads (**Figure 1**). The general loading corresponds to tension  $\sigma_{22}^a$  and shears  $\sigma_{21}^a$  and  $\sigma_{23}^a$  along  $x_2$ ,  $x_1$  and  $x_3$ , respectively, with associated induced normal Poisson's stresses  $-\nu_A(j)\sigma_{22}^a$  along  $x_1$  ( $j=1$ ) and  $x_3$  ( $j=3$ ). The nucleus has been represented by a continuous distribution of infinitesimal elliptic dislocation loops. Equilibrium dislocation distributions, boundary front stresses and extension force  $G$  per unit length have been expressed.  $Ox'_2$  is a symmetrical axis of the crack nuclei. In  $x'_1x'_3$  - planes the bases are elliptical, with semiaxes  $\rho_1$  and  $\rho_2$  along  $x'_1$  and  $x'_3$ , such that  $a_r = \rho_1 / \rho_2 = \text{constant}$  about any elevation  $x'_2 = OO' \equiv h$  along  $Ox'_2$ . The running position  $P_D (x'_1, x'_2, x'_3)$  at the elevation  $h$  along the base is written with respect to ( $O; x'_j$ ) as

$$\overline{OP}_D = \begin{pmatrix} x'_1 = \rho \sin \phi \\ x'_2 = h = \rho_1 \tan \theta \\ x'_3 = \rho \cos \phi \end{pmatrix}; \quad -\pi \leq \phi \leq \pi, \quad 0 \leq \theta < \pi/2;$$

$$\rho^2 = \rho_1^2 / (\sin^2 \phi + a_r^2 \cos^2 \phi). \quad (1)$$

The angle  $\phi$  is between  $O'x'_3$  and  $O'P_D$  as shown in **Figure 1**. Angle  $\theta$  is measured in  $Ox'_1x'_2$  between  $\mathbf{P}_D (\phi = \pi/2) \mathbf{O}'$  and  $\mathbf{P}_D (\phi = \pi/2) \mathbf{O}$  where  $P_D$

( $\phi = \pi/2$ ) has elevation  $x'_2 = h$  from  $O x'_1 x'_3$ ; its alternate interior angle is shown in **Figure 1**. Additional angular parameters  $\theta_0$  and  $\phi_0$  (Euler's angles) are introduced that connect  $\bar{x}_j$  to  $\bar{x}'_j$ .

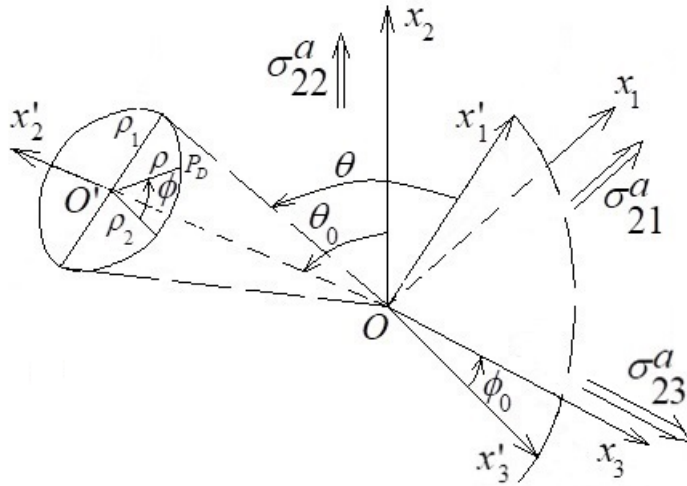


**Figure 1 :** Elliptical base (elevation  $x'_2 = OO' \equiv h$ ) of the conoidal crack with semi-axes  $\rho_1$  and  $\rho_2$  along  $x'_1$  and  $x'_3$ . The running point  $P_D$  (1) along the base and angular parameters  $\theta_0$  and  $\phi_0$  that connect  $x_j$  and  $\bar{x}'_j$  are illustrated. Angle  $\theta$  is introduced by the relation  $\tan \theta = OO' / \rho_1$ . The medium suffers uniformly applied tension  $\sigma_{22}^a$  in the vertical  $x_2$  - direction and shears  $\sigma_{21}^a$  and  $\sigma_{23}^a$  (parallel to the horizontal  $x_1x_3$ -plane) in the  $x_1$  and  $x_3$  directions.

In the second part (*Part II*) of this study [2], the treatment in [1] with associated model (**Figure 1**) is applied to high temperature mechanical twinning systems  $TS = [\eta_1] (K_1)$  ( $\eta_1$  and  $K_1$  being the twinning direction and plane, respectively) observed in [112] copper single crystals deformed at constant strain rates. Primary close-packed twinning plane  $(1\bar{1}1) = K_1(a - c)$  with associated twinning directions,  $\eta_1(a) = [121]$ ,  $\eta_1(b) = [21\bar{1}]$  and  $\eta_1(c) = [1\bar{1}2]$ , and the cross-slip  $(11\bar{1}) = K_1(d)$  plane with twinning direction  $\eta_1(d) = [112]$  (**Figure 2**) are considered. Graphical plots of  $\langle G \rangle$  as a function of  $\theta_0$  and  $\phi_0$ , are displayed. Positive local  $\langle G \rangle$  maxima are observed for these twinning systems (except  $TS(c)$ ) suggesting that these correspond to equilibrium configurations, in agreement with experiments. Equilibrium states during evolution are those observed over large time intervals and propagation

distances. In summary,  $1/6 \langle 112 \rangle \{111\}$  twinning corresponds to positive  $\langle G \rangle$  maxima in copper. In this *part III*, the treatment in [1] with associated model (**Figure 1**) is used to find possible fracture systems  $FS = [T] (F)$  ( $T$  and  $F$  being the fracture direction and plane, respectively) in  $\text{CoSi}_2$  single crystals. In *Section 2*, the methodology of the treatment is described. In *Section 3*, graphical representations of  $\langle G \rangle$  are displayed corresponding to different fracture systems. *Section 4* and *5* are devoted to discussion and conclusion, respectively.

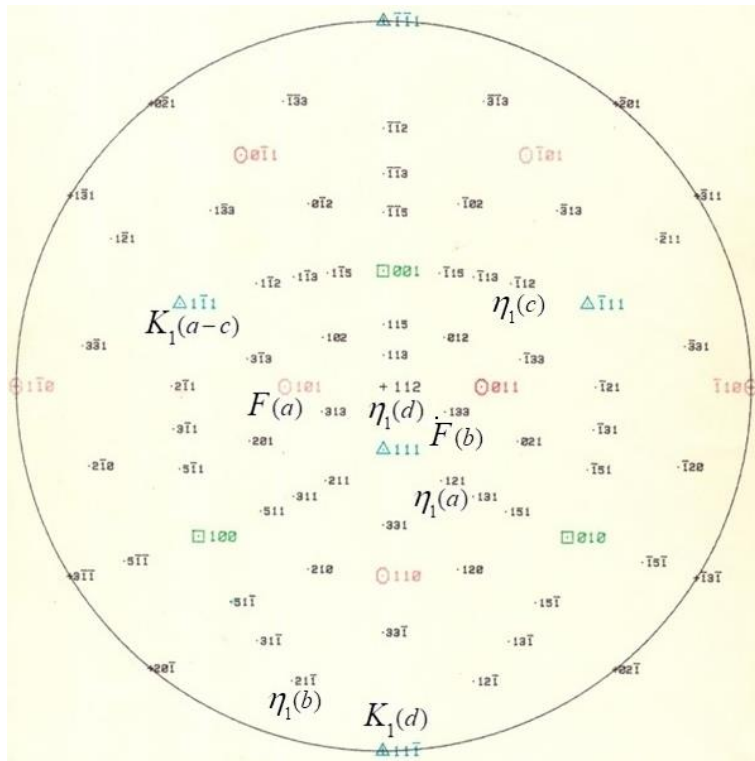


**Figure 2 :** Stereographic projection with centre  $[112]$  for the identification of cracking and twinning systems

## II - METHODOLOGY

**Figure 1** is used to specify a plane of fracture ( $F$ ).  $x_2$  is vertical, parallel to the applied tension,  $x_3$  is then determined as the intersection between ( $F$ ) and the laboratory horizontal plane  $(x_2) = O x_1 x_3$  allowing  $x_1$  to be known. For definiteness,  $x_2$  is fixed to  $[112]$  and we seek possible fracture systems under such conditions. Then graphical plots of  $\langle G \rangle$  as a function of  $\phi_0$  are displayed. The crack propagation directions  $[T]$  in ( $F$ ) are those associated to positive local maxima. It is assumed that the friction stresses are zero. The results for the  $\{111\}$  fractures are those of the twinning systems  $TS(i)$  mentioned earlier in

Section 1. Additional fracture planes ( $F(j), j= a$  and  $b$ ) considered are:

(1)  $F(a) = (101)$ : using **Figures 1** and **2** and indicating the directions only, we have  $\theta_0 = 30^\circ, x_2 = [112], x_3 = [11\bar{1}], x_1 = [\bar{1}10], x'_2 = [101]$

(2)  $F(b) = (122)$ :  $\theta_0 = 18^\circ, x_2 = [112], x_3 = [\bar{4}02], x_1 = [1\bar{5}2], x'_2 = [122]$   
(2)

For  $\text{CoSi}_2, C_{11} = 2.16, C_{12} = 1.35$  and  $C_{44} = 0.81$  in units of  $[10^{11} \text{ N/m}^2]$ , taken from [3].  $M_{12} = \sigma_{21}^a / \sigma_{22}^a, M_{13} = \sigma_{23}^a / \sigma_{22}^a, \nu_A(1) = \nu_A(3) = 1/3, a_r = 4/3.$

### III - RESULTS

Again, we consider average  $\langle G \rangle$  obtained in the first part of this study (see relation (34) of [1]) and present below graphical plots of its normalized value  $\langle \tilde{G} \rangle$  defined as

$$\langle \tilde{G} \rangle = \langle G \rangle / G_C^I = \langle \tilde{G} \rangle (\theta, \theta_0, \phi_0, M_{12}, M_{13}, a_r, C_{mm}),$$

$$G_C^I = \frac{2^5 \alpha_0^2 a_r^4}{3\pi^2 C_{44}} (K_I^0)^2; \tag{3}$$

where  $K_I^0 = \sigma_{22}^a \sqrt{\pi a_1}$ . Octahedral fracture systems are invariably of the type  $\langle 112 \rangle \{111\}$  as for the twinning systems and examples correspond to  $\eta_1[a-d] K_1 [a-d]$  of **Figure 2** [2]. Fracture plane  $F(a) = (101)$  is further considered and **Figures 3** and **4** are displayed in  $\text{CoSi}_2$  material. Positive maxima of  $\langle \tilde{G} \rangle$  are at  $\phi_0 = 60^\circ$  and  $10^\circ$  approximately, respectively; these correspond to systems  $[13\bar{1}](101)$  and  $[\bar{1}31](101)$ .

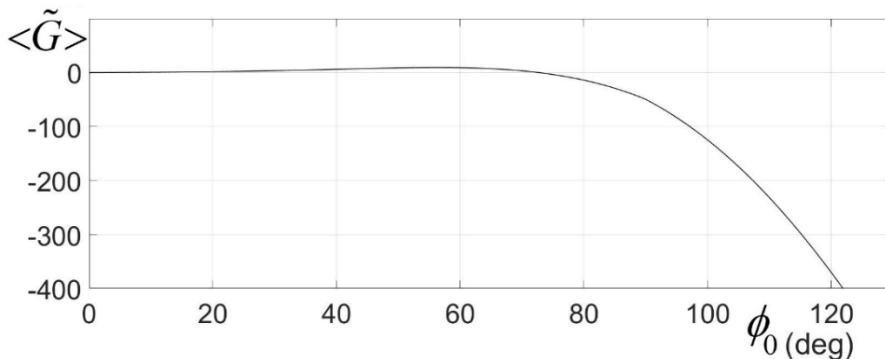


**Figure 3 :**  $\langle \tilde{G} \rangle$  (3) as a function of  $\phi_0$  for  $\theta = \pi/3$  and  $\theta_0 = 30^\circ$ . This corresponds to the fracture system  $[13\bar{1}](101)$  ( $\phi_0 = 60^\circ$ ).

$M_{12} = M_{13} = 10^{-4}, \nu_A(1) = \nu_A(3) = 1/3, a_r = 4/3, \text{CoSi}_2$  material.

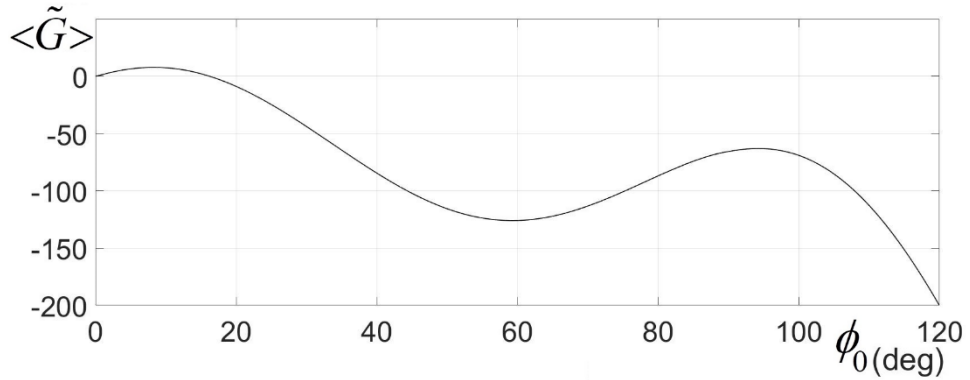


**Figure 4 :**  $\langle \tilde{G} \rangle$  (3) as a function of  $\phi_0$  for  $\theta = \pi / 3$  and  $\theta_0 = 30^\circ$ . This corresponds to the fracture system  $[\bar{1}31](101)$  ( $\phi_0 = 10^\circ$ ).  $M_{12} = 1$ ,  $M_{13} = 10^{-4}$   $\nu_A(1) = \nu_A(3) = 1/3$ ,  $a_r = 4/3$ ,  $CoSi_2$  material.

Consideration is also given to the fracture plane (122) =  $F(b)$  (Figures 5 and 6). Positive maxima of  $\langle \tilde{G} \rangle$  are at  $\phi_0 = 50^\circ$  and  $110^\circ$ , corresponding to  $[\bar{2}23](122)$  and  $[\bar{4}11](122)$ , respectively.

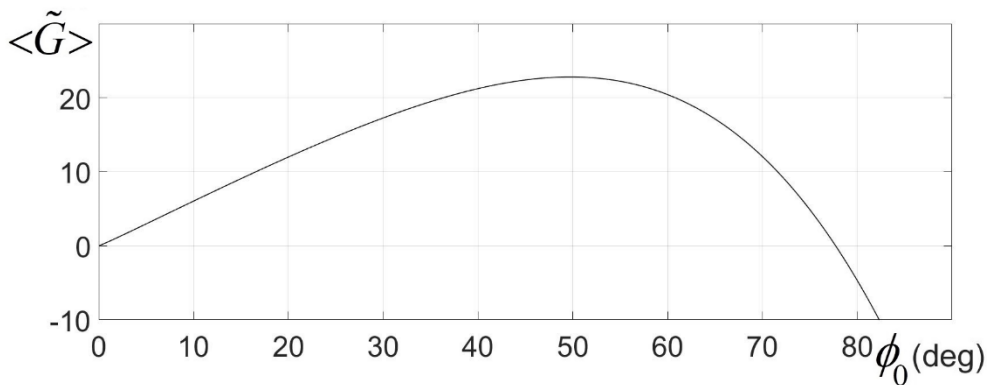


**Figure 5 :**  $\langle \tilde{G} \rangle$  (3) as a function of  $\phi_0$  for  $\theta = \pi / 3$  and  $\theta_0 = 18^\circ$ . This corresponds to the fracture system  $[\bar{2}23](122)$  ( $\phi_0 = 50^\circ$ ).  $M_{12} = M_{13} = 10^{-4}$ ,  $\nu_A(1) = \nu_A(3) = 1/3$ ,  $a_r = 4/3$ ,  $CoSi_2$  material.

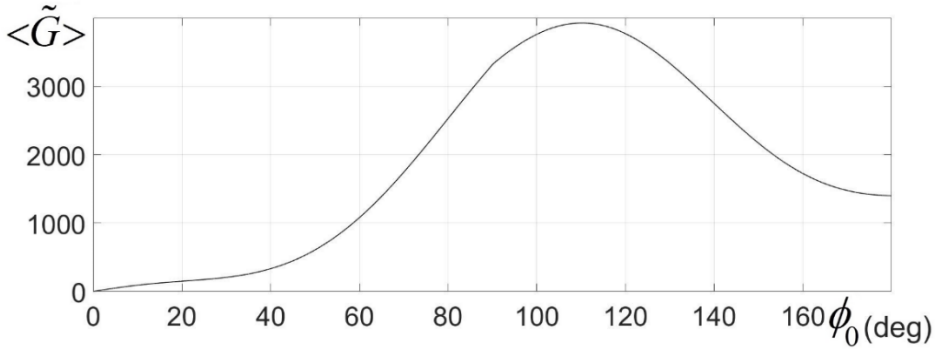


**Figure 6 :**  $\langle \tilde{G} \rangle$  (3) as a function of  $\phi_0$  for  $\theta = \pi / 3$  and  $\theta_0 = 18^\circ$ . This corresponds to the fracture system  $[\bar{4}11](122)$  ( $\phi_0 = 110^\circ$ ).  $M_{12} = 4$ ,  $M_{13} = 10^{-4}$   $\nu_A(1) = \nu_A(3) = 1/3$ ,  $a_r = 4/3$ , CoSi<sub>2</sub> material.

It is stressed that  $\langle 110 \rangle$  is not a fracture propagation direction in the fracture planes investigated. Also increasing the shearing stress  $M_{13}$  reduces  $\langle \tilde{G} \rangle$  to negative values; this means that this stress works against the expansion of the cracks.

#### IV - DISCUSSION

The experimental works on CoSi<sub>2</sub> [3 – 6] will serve for confrontation. Fractures on close-packed octahedral planes  $\{111\}$  have invariably a  $\langle 112 \rangle$  propagation direction [4 – 6]. In [113] CoSi<sub>2</sub> single crystals deformed under compression up to brittle fracture, the fracture system is  $[112] (11\bar{1}) = \eta_1(d) K_1(d)$ , **Figure 2** : this is clearly shown on the micrograph (see *Fig. 2a* of [5]). Agreement between theory and experiment is complete. Twinning and fracture systems are the same  $\langle 112 \rangle \{111\}$ . The theory is describing twinning and fracture by representing these with continuous distributions of Volterra infinitesimal dislocations. Fractures on  $(101)$  [4, 6] suggest that the direction of fracture propagation is  $[13\bar{1}]$  (see *Fig.4* of [4] and *Table 1* there for the numerous number of specimens involved). This is confirmed by the present analysis (**Figure 3**). Increasing the shearing stress  $M_{12}$  (**Figure 4**) provokes a change in the fracture propagation direction to  $[\bar{1}31]$ . Hence  $\langle 113 \rangle$  seems the crack propagation direction in  $\{101\}$  planes. Fractures on  $(212)$  [4, 6] clearly indicate that the fracture propagation direction is  $[\bar{1}4\bar{1}]$ . **Figure 6** has predicted the cracking system  $[\bar{4}11] (122)$  for sufficiently large  $M_{12} = 4$ . For small shearing stresses, **Figure 5** suggests the system  $[\bar{2}23] (122)$ . Increasing  $M_{13}$  works against crack expansion. This is because  $\sigma_{23}^a$  in the modelling (**Figure 1**) lies parallel to the elliptic crack front. This negative role has been mentioned earlier [7]. **V - CONCLUSION**

Brittle fracture systems ( $\langle 112 \rangle \{111\}$ ,  $\langle 113 \rangle \{110\}$ ,  $\langle 411 \rangle \{122\}$ ) observed in  $\text{CoSi}_2$  single crystals [3 – 6] have been confronted to the theoretical analysis of Part I of this study [1]. These do correspond to positive local average  $\langle G \rangle$  maxima, where the quantity  $\langle G \rangle$  is the crack extension force  $G$  per unit length of the crack front, averaged over all the positions on the crack front. Hence, equilibrium crack systems provided by the theory are those observed experimentally. Both twinning [2] and cracking systems are of the type  $\langle 112 \rangle \{111\}$  as expected. It is understood that above results are achieved within the framework of the theory of linear elasticity incorporating dislocations as crystal defects and basic elements in the mathematical treatment of fracture.

## REFERENCES

- [1] - P. N. B. ANONGBA, Conoidal crack with elliptic bases, within cubic crystals, under arbitrarily applied loadings – I. Dislocations, crack-tip stress and crack extension force, (a) *Rev. Ivoir. Sci. Technol.*, 43 (2024) 100 - 121; (b) *ResearchGate*, DOI: 10.13140/RG.2.2.21165.67044
- [2] - P. N. B. ANONGBA, Conoidal crack with elliptic bases, within cubic crystals, under arbitrarily applied loadings – II. Application to mechanical twinning of [112] copper single crystals, (a) *Rev. Ivoir. Sci. Technol.*, 43 (2024) 122 - 131; (b) *ResearchGate*, DOI: 10.13140/RG.2.2.33154.70085
- [3] - P. N. B. ANONGBA and S.G. STEINEMANN, Dislocations and plasticity in [113]  $\text{CoSi}_2$  single crystals between room temperature and 1173 K, *phys. stat. sol. (a)*, 140 (1993) 391 - 409
- [4] - P. N. B. ANONGBA, S. OBERLI and S.G. STEINEMANN, A study of the brittle fracture characteristics of  $\text{CoSi}_2$  using laser beam reflections, *Acta metal. Mater.* 43 (1995) 2275 - 2285
- [5] - P. N. B. ANONGBA and S.G. STEINEMANN, Slip systems and microstructures in plastically deformed [113]  $\text{CoSi}_2$  single crystals, Proceedings of the 10<sup>th</sup> International Conference of the Strength of Materials (ICSMA – 10), Sendai, Japan (1994) 125 - 128
- [6] - P. N. B. ANONGBA, S. OBERLI and S.G. STEINEMANN, Brittle fracture mechanisms of  $\text{CoSi}_2$  single crystals at room temperature, Proceedings of the 10<sup>th</sup> International Conference of the Strength of Materials (ICSMA - 10), Sendai, Japan, (1994) 431 - 434
- [7] - P. N. B. ANONGBA, Elliptical crack under arbitrarily applied loadings : dislocation, crack-tip stress and crack extension force, *Rev. Ivoir. Sci. Technol.*, 38 (2021) 388 - 409